

$[\text{Ag}_2(\text{aca})_2]_n$ and $[\text{Ag}_4(\text{aca})_4(\text{NH}_3)_2]$ (acaH = 9-anthracenecarboxylic acid): Synthesis, X-ray crystal structures, antimicrobial and anti-cancer activities

Robert Curran^a, Joanne Lenehan^a, Malachy McCann^{a,*}, Kevin Kavanagh^b,
Michael Devereux^c, Denise A. Egan^d, Grace Clifford^d, Kevin Keane^d,
Bernadette S. Creaven^d, Vickie McKee^e

^a Chemistry Department, National University of Ireland Maynooth, Maynooth, Co. Kildare, Ireland

^b Biology Department, National University of Ireland Maynooth, Maynooth, Co. Kildare, Ireland

^c Dublin Institute of Technology, Cathal Brugha Street, Dublin 2, Ireland

^d Centre for Pharmaceutical Research and Development (CPRD), Institute of Technology, Tallaght, Dublin 24, Ireland

^e Chemistry Department, Loughborough University, Loughborough, Leics., LE11 3TU, UK

Received 12 June 2007; accepted 26 June 2007

Available online 5 July 2007

Abstract

$[\text{Ag}_2(9\text{-aca})_2]_n$ and $[\text{Ag}_4(9\text{-aca})_4(\text{NH}_3)_2]$ (9-acaH = 9-anthracenecarboxylic acid) have been prepared and structurally characterized. $[\text{Ag}_2(9\text{-aca})_2]_n$ consists of polymeric ribbons of linked disilver(I) syn–syn bridged dicarboxylate units. $[\text{Ag}_4(9\text{-aca})_4(\text{NH}_3)_2]$ is tetrameric and centrosymmetric, with two syn–syn bridging carboxylates linked to the bimetallic Ag–Ag core and a further two syn–anti bridged carboxylate ligands in the equatorial plane, being coordinated to one Ag in the bimetallic core and to a second Ag, with the latter also bonded to an NH_3 ligand. *In vitro* studies show that both complexes are extremely cytotoxic against selected human fungal and bacterial pathogens, and each complex also greatly inhibits the growth of two mammalian cancer cell lines.

© 2007 Elsevier B.V. All rights reserved.

Keywords: 9-Anthracenecarboxylic acid; X-ray structure; Silver(I); Anti-fungal; Anti-bacterial; Anti-cancer

In the early part of the last century elemental silver and simple silver salts were used as antimicrobial agents in curative and preventative healthcare, but lost favour following the discovery of penicillin and other new antibiotics. However, silver-based chemotherapy is now undergoing somewhat of a renaissance, instigated primarily by the emergence of stubborn microbial strains that are extremely tolerant of current prescription drugs (for example, methicillin-resistant *Staphylococcus aureus* (MRSA)). We have recently demonstrated the *in vitro* efficacy of a range of Ag(I) complexes against fungal and bacterial opportunistic human pathogens [1–3] and also against mammalian can-

cer cells [4–6]. Herein, we detail the synthesis and structures of two new Ag(I) complexes of 9-anthracenecarboxylic acid (9-acaH) and also report the growth inhibitory effects of the complexes on harmful bacteria (MRSA and *Escherichia coli*) and fungi (*Candida albicans*). In addition, the anti-cancer chemotherapeutic potential of the complexes was determined using two human-derived cell lines (hepatocellular carcinoma (Hep-G₂) and kidney adenocarcinoma (A-498)).

Ag_2O reacted with 9-acaH (1:2 mol ratio) to form $[\text{Ag}_2(9\text{-aca})_2]_n$, whilst AgNO_3 combined with 9-acaH (1:1 mol ratio) in the presence of ammonia to yield the ammine adduct $[\text{Ag}_4(9\text{-aca})_4(\text{NH}_3)_2]$ [7]. X-ray diffraction analysis [8] revealed that $[\text{Ag}_2(9\text{-aca})_2]_n$ consists of polymeric ribbons of linked disilver(I) dicarboxylate units

* Corresponding author. Tel.: +353 1 7083767; fax: +353 1 7083815.
E-mail address: malachy.mccann@nuim.ie (M. McCann).

(Fig. 1, Table 1) and is structurally similar to simpler silver(I) carboxylates [10]. The Ag1–Ag1A distance is 2.8508(9) Å and indicates some metal–metal interaction. The carboxylate ligands are syn–syn bridging to the bimetallic core and this is further linked to neighbouring cores by weaker equatorial Ag–O interactions. There are two independent Ag(9-aca) units in the asymmetric unit, generating two independent ribbons which differ principally in the angle of the anthracene unit to the ribbon. Both types of ribbon run parallel to the b-axis (Fig. 2). The longer Ag...Ag distances in the structure (e.g. Ag1...Ag1b) are

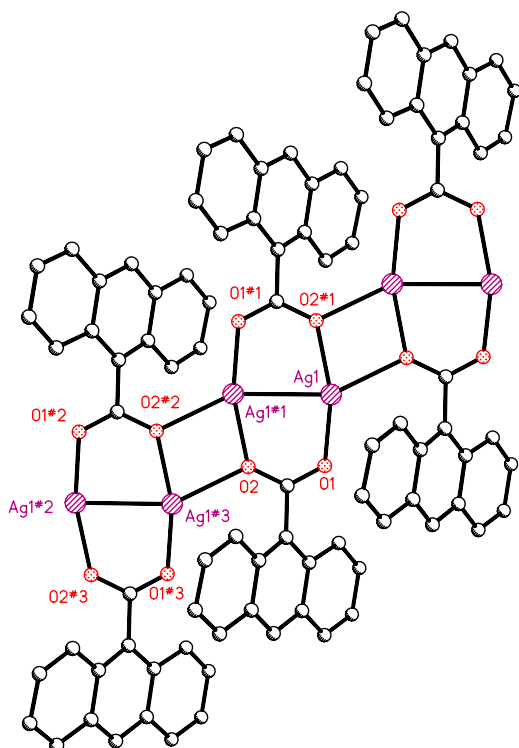


Fig. 1. Structure of one of the polymeric strands in $[\text{Ag}_2(9\text{-aca})_2]_n$. Symmetry transformations used to generate equivalent atoms: #1 $-x+1, -y+1, -z$; #2 $x, y+1, z$; #3 $x, y-1, z$.

3.657(1) and 3.615(1) Å for the Ag1 and Ag2 chains, respectively.

$[\text{Ag}_4(9\text{-aca})_4(\text{NH}_3)_2]$ is tetrameric and centrosymmetric (Fig. 3, Table 2) and has a slightly longer Ag1–Ag1A distance (2.939(1) Å). Again, the two carboxylates which are linked to the metal–metal bonded bimetallic core are syn–syn bridging. The two carboxylate ligands in the equatorial plane are in the syn–anti configuration being coordinated to one Ag in the bimetallic core and to a second silver (Ag2). The Ag1–Ag2 distance is 3.63 Å. Whilst Ag2 is coordinated approximately linearly by carboxylate and ammonia it also interacts with the π -systems of a neighbouring molecule, and this interaction is supported by two long H-bonds from the ammonia ligand to carboxylate oxygen atoms of the same neighbouring molecule (Fig. 4). This arrangement leads to the packing arrangement seen in Fig. 5, which is notably more detailed than that for $[\text{Ag}_2(9\text{-aca})_2]_n$.

Whilst 9-anthracenecarboxylic acid was inactive against fungi and bacteria at a concentration of 225 μM , both $[\text{Ag}_2(9\text{-aca})_2]_n$ and $[\text{Ag}_4(9\text{-aca})_4(\text{NH}_3)_2]$ demonstrated high cytotoxicity *in vitro* [11] (Table 3). $[\text{Ag}_4(9\text{-aca})_4(\text{NH}_3)_2]$ was over 30 times more active against *C. albicans* than the commonly used antifungal agent ketoconazole.

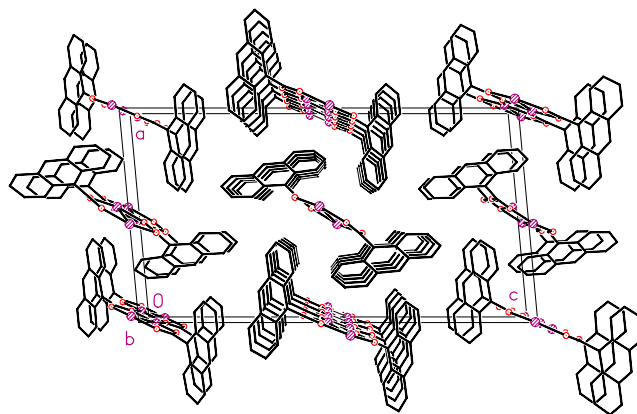


Fig. 2. Packing diagram for $[\text{Ag}_2(9\text{-aca})_2]_n$.

Table 1

Selected bond lengths [Å] and angles [°] for $[\text{Ag}_2(9\text{-aca})_2]_n$

Ag(1)–O(1)	2.170(3)	Ag(2)–O(3)	2.190(3)
Ag(1)–O(2)#1	2.190(3)	Ag(2)–O(4)#4	2.243(3)
Ag(1)–O(2)#2	2.473(4)	Ag(2)–O(4)#3	2.381(4)
Ag(1)–Ag(1)#1	2.8508(9)	Ag(2)–Ag(2)#4	2.8643(9)
O(2)–Ag(1)#1	2.190(3)	O(4)–Ag(2)#4	2.243(3)
O(2)–Ag(1)#3	2.473(4)	O(4)–Ag(2)#2	2.381(4)
O(1)–Ag(1)–O(2)#1	162.20(13)	O(3)–Ag(2)–O(4)#4	163.19(13)
O(1)–Ag(1)–O(2)#2	116.66(12)	O(3)–Ag(2)–O(4)#3	119.35(12)
O(2)#1–Ag(1)–O(2)#2	76.88(13)	O(4)#4–Ag(2)–O(4)#3	77.20(13)
O(1)–Ag(1)–Ag(1)#1	84.41(9)	O(3)–Ag(2)–Ag(2)#4	84.01(9)
O(2)#1–Ag(1)–Ag(1)#1	79.04(9)	O(4)#4–Ag(2)–Ag(2)#4	79.39(9)
O(2)#2–Ag(1)–Ag(1)#1	150.72(8)	O(4)#3–Ag(2)–Ag(2)#4	156.59(8)
Ag(1)#1–O(2)–Ag(1)#3	103.12(13)	Ag(2)#4–O(4)–Ag(2)#2	102.80(13)

Symmetry transformations used to generate equivalent atoms: #1 $-x+1, -y+1, -z$; #2 $x, y+1, z$; #3 $x, y-1, z$; #4 $-x, -y+2, -z+1$.

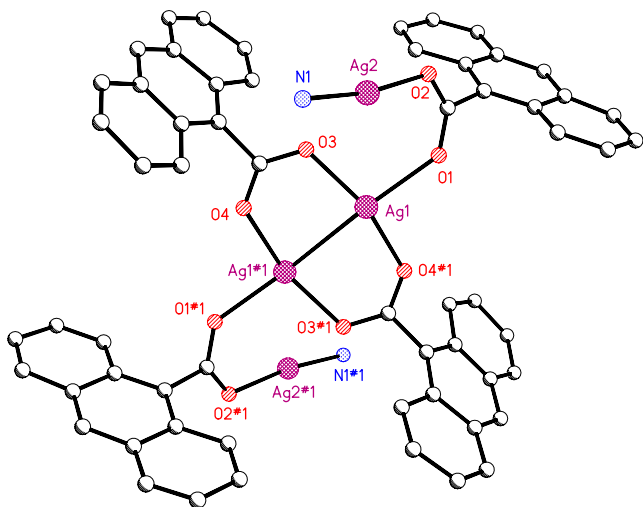


Fig. 3. X-ray crystal structure of $[\text{Ag}_4(9\text{-aca})_4(\text{NH}_3)_2]$. Symmetry transformations used to generate equivalent atoms: #1 $-x + 1, -y, -z$.

Table 2

Selected bond lengths [\AA] and angles [$^\circ$] for $[\text{Ag}_4(9\text{-aca})_4(\text{NH}_3)_2]$

Ag(1)–O(3)	2.193(5)	Ag(1)–Ag(1)#1	2.9390(13)
Ag(1)–O(4)#1	2.260(5)	Ag(2)–O(2)	2.134(5)
Ag(1)–O(1)	2.328(6)	Ag(2)–N(1)	2.147(6)
O(3)–Ag(1)–O(4)#1	155.66(18)	O(4)#1–Ag(1)–Ag(1)#1	75.26(13)
O(3)–Ag(1)–O(1)	100.5(2)	O(1)–Ag(1)–Ag(1)#1	164.10(16)
O(4)#1–Ag(1)–O(1)	95.07(19)	O(2)–Ag(2)–N(1)	170.5(2)
O(3)–Ag(1)–Ag(1)#1	85.16(14)		

Symmetry transformations used to generate equivalent atoms: #1 $-x + 1, -y, -z$.

Although $[\text{Ag}_2(9\text{-aca})_2]_n$ appears to be only half as active as $[\text{Ag}_4(9\text{-aca})_4(\text{NH}_3)_2]$, when their MIC_{100} values are equated to their silver ion content (58 μM and 56 μM , respectively) then both complexes display approximately equal activity.

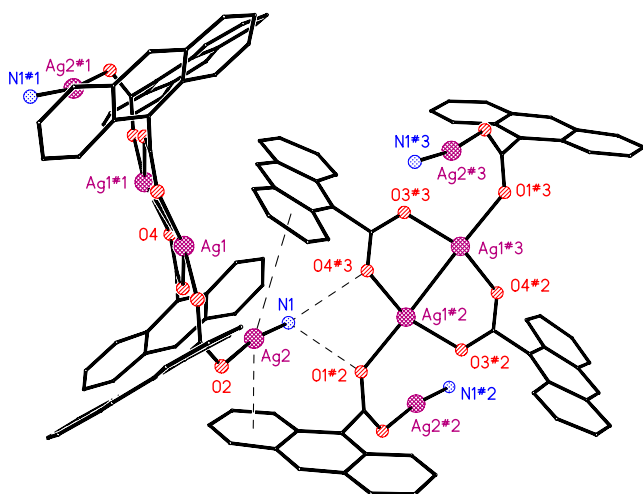


Fig. 4. Intermolecular π - and H-bonding interactions in $[\text{Ag}_4(9\text{-aca})_4(\text{NH}_3)_2]$. Symmetry transformations used to generate equivalent atoms: #1 $-x + 1, -y, -z$; #2 $x, -y + 1/2, z + 1/2$; #3 $-x + 1, y + 1/2, -z + 1/2$.

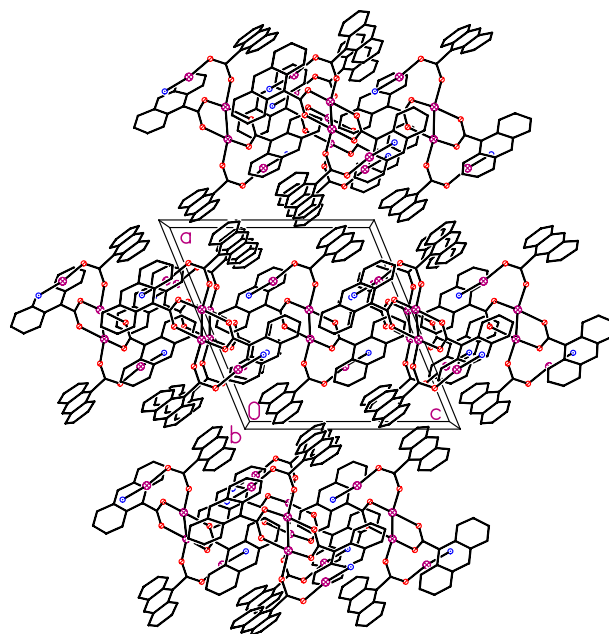


Fig. 5. Packing diagram for $[\text{Ag}_4(9\text{-aca})_4(\text{NH}_3)_2]$.

Against MRSA and *E. coli* $[\text{Ag}_2(9\text{-aca})_2]_n$ and $[\text{Ag}_4(9\text{-aca})_4(\text{NH}_3)_2]$ both appeared to perform significantly better than the topical antibacterial agent silver(I) sulfadiazine. However, when equated to their silver ion content all three Ag(I) complexes were equally active.

The anti-cancer chemotherapeutic potential of $[\text{Ag}_2(9\text{-aca})_2]_n$ and $[\text{Ag}_4(9\text{-aca})_4(\text{NH}_3)_2]$ was determined against the human-derived cell lines, hepatocellular carcinoma (Hep-G₂) and kidney adenocarcinoma (A-498), and compared to the Pt(II) complex, cisplatin [13] (Table 3). Each of the Ag(I) complexes decreased the proliferation of both cancer cell lines in a concentration-dependent manner. $[\text{Ag}_4(9\text{-aca})_4(\text{NH}_3)_2]$ was the most active of the anthracene complexes, suggesting that the extra two Ag(I) centres and/or the additional two NH_3 ligands were augmenting the activity. In our previous studies using $[\text{Ag}_2(\text{salH})_2]$ and $[\text{Ag}_2(\text{NH}_3)_2(\text{salH})_2]$ [4], the latter ammine complex was more active against Hep-G₂ but less potent against A-498. In comparison, $[\text{Ag}_4(9\text{-aca})_4(\text{NH}_3)_2]$ was more cytotoxic than $[\text{Ag}_2(\text{salH})_2]$, $[\text{Ag}_2(\text{NH}_3)_2(\text{salH})_2]$ and cisplatin across both cell lines. Finally, hepatic cells appeared to be more sensitive to the effects of $[\text{Ag}_4(9\text{-aca})_4(\text{NH}_3)_2]$ than

Table 3

Antimicrobial and anti-cancer activities (μM concentrations)

Drug	<i>C. albicans</i> MIC_{100}	MRSA MIC_{50}	<i>E. coli</i> MIC_{50}	Hep-G ₂ IC_{50}	A-498 IC_{50}
$[\text{Ag}_2(9\text{-aca})_2]_n$	0.29	55.91	61.53	27.8	30.0
$[\text{Ag}_4(9\text{-aca})_4(\text{NH}_3)_2]$	0.14	28.36	40.73	3.6	5.5
Ketoconazole	4.70				
Silver(I) sulfadiazine		120.40	154.00		
Cisplatin				15.0	14.0

renal cells, suggesting a degree of anti-cancer cyto-selectivity.

Acknowledgements

Financial support from the Irish Research Council for Science, Engineering and Technology (IRCSET) and the John and Pat Hume Scholarship Scheme, NUI Maynooth (R. Curran) are gratefully acknowledged. We thank the CCLRC for access to station 16.2 of the SRS at Daresbury.

Appendix A. Supplementary material

CCDC 626868 and 605749 contain the supplementary crystallographic data for $[\text{Ag}_2(9\text{-aca})_2]_n$ and $[\text{Ag}_4(9\text{-aca})_4(\text{NH}_3)_2]$. These data can be obtained free of charge via <http://www.ccdc.cam.ac.uk/conts/retrieving.html>, or from the Cambridge Crystallographic Data Centre, 12 Union Road, Cambridge CB2 1EZ, UK; fax: (+44) 1223-336-033; or e-mail: deposit@ccdc.cam.ac.uk. Supplementary data associated with this article can be found, in the online version, at [doi:10.1016/j.inoche.2007.06.021](https://doi.org/10.1016/j.inoche.2007.06.021).

References

- [1] R. Rowan, T. Tallon, A.M. Sheahan, R. Curran, M. McCann, K. Kavanagh, M. Devereux, V. McKee, *Polyhedron* 25 (2006) 1771.
- [2] B.S. Creaven, D.A. Egan, K. Kavanagh, M. McCann, A. Noble, B. Thati, M. Walsh, *Inorg. Chim. Acta* 359 (2006) 3976.
- [3] B. Thati, A. Noble, R. Rowan, B.S. Creaven, M. Walsh, M. McCann, D. Egan, K. Kavanagh, *Toxicol. In Vitro* 21 (2007) 801.
- [4] B. Coyle, M. McCann, K. Kavanagh, M. Devereux, V. McKee, N. Kayal, D. Egan, C. Deegan, G.J. Finn, *J. Inorg. Biochem.* 98 (2004) 1361.
- [5] M. McCann, B. Coyle, S. McKay, P. McCormack, K. Kavanagh, M. Devereux, V. McKee, P. Kinsella, R. O'Connor, M. Clynes, *BioMetals* 17 (2004) 635.
- [6] C. Deegan, M. McCann, M. Devereux, B. Coyle, D.A. Egan, *Cancer Lett.* 247 (2007) 224.
- [7] All preparations were conducted in the absence of light and samples were stored in the dark. $[\text{Ag}_2(9\text{-aca})_2]_n$: Ag_2O (0.70 g, 3.0 mmol) was suspended in ethanol and added to a refluxing solution of 9-anthracenecarboxylic acid (9-acaH) (1.332 g, 6.0 mmol) in ethanol (170 cm^3). A green precipitate formed and the suspension was refluxed for 1 h. The solid was filtered off and placed in refluxing ethanol (350 cm^3) for 1 h. A brown precipitate was filtered off and the filtrate reduced to low volume to yield a yellow solid. The yellow solid was filtered off, washed with cold ethanol and allowed to air-dry. Yield: 0.41 g, 21%. The yellow complex was insoluble in water, soluble in hot ethanol and hot toluene, and soluble in DMSO, chloroform and acetonitrile. Crystals suitable for X-ray structural analysis were obtained by recrystallisation from hot ethanol. Elemental analysis calcd (%) for $\text{C}_{30}\text{H}_{18}\text{O}_4\text{Ag}_2$: C, 54.74; H, 2.76. Found: C, 54.08; H, 2.68. IR (KBr): 3384 cm^{-1} , 3047, 1566, 1537, 1429, 1391, 1319. ^1H NMR (DMSO- d_6): 7.47 ppm (m), 8.03 (m), 8.44 (s). $[\text{Ag}_4(9\text{-aca})_4(\text{NH}_3)_2]$: AgNO_3 (0.51 g, 3.0 mmol) was dissolved in water (5 cm^3) and concentrated ammonia solution (ca. 10 cm^3 , density 0.88 g cm^{-3}) was added until all solids dissolved. This solution was then added to a solution of 9-anthracenecarboxylic acid (9-acaH) (0.67 g, 3.0 mmol) in ethanol:water (80:20, 100 cm^3) and more concentrated ammonia added (10 cm^3 slowly with stirring). The resulting solution was stirred for 0.5 h and then rotary evaporated to low volume. The precipitated light yellow solid was filtered off, washed with cold ethanol and allowed to air-dry. Yield: 0.46 g, 45%. Over a period of a few days some light-yellow crystals deposited in the filtrate and these were used for X-ray studies. The original reaction filtrate was allowed to slowly evaporate over a period of days to give light-yellow crystals suitable for X-ray structural analysis. The complex was insoluble in water, slightly soluble in warm ethanol and warm acetonitrile and soluble in DMSO. Elemental analysis calcd (%) for $\text{C}_{60}\text{H}_{42}\text{N}_2\text{O}_8\text{Ag}_4$: C, 53.36; H, 3.14; N, 2.07. Found: C, 53.2; H, 3.03; N, 2.12. IR (KBr): 3410 cm^{-1} , 3050, 1558, 1428, 1390, 1319. ^1H NMR (DMSO- d_6): 3.04 ppm (s), 7.47 (m), 8.08 (m), singlet 8.44 (s).
- [8] Crystal data for $[\text{Ag}_4(9\text{-aca})_2]_n$: monoclinic, $P2_1/c$, $a = 14.813(3)$ Å, $b = 5.6055(12)$ Å, $c = 27.413(6)$ Å, $\alpha = 90^\circ$, $\beta = 95.250(3)^\circ$, $\gamma = 90^\circ$, $V = 2266.6(8)$ Å 3 , $Z = 4$, $R[I > 2\sigma(I)]$ 0.0374 and 0.0854. Crystal data for $[\text{Ag}_4(9\text{-aca})_4(\text{NH}_3)_2]$: monoclinic, $P2_1/c$, $a = 16.837(3)$ Å, $b = 9.8639(16)$ Å, $c = 16.035(3)$ Å, $\alpha = 90^\circ$, $\beta = 112.383(2)^\circ$, $\gamma = 90^\circ$, $V = 2462.4(7)$ Å 3 , $Z = 2$, $R[I > 2\sigma(I)]$ 0.0494 and 0.1071. Data for $[\text{Ag}_4(9\text{-aca})_2]_n$ were collected on a Bruker APEX II diffractometer ($\lambda = 0.71073$ Å, $T = 150(2)$ K), whilst data for $[\text{Ag}_4(9\text{-aca})_4(\text{NH}_3)_2]$ were collected at 150(2) K on station 16.2 of the SRS at Daresbury ($\lambda = 0.84620$ Å, 150(2) K). Both structures were solved by direct methods and refined on F^2 using all the reflections [9]. All the non-hydrogen atoms were refined using anisotropic atomic displacement parameters and hydrogen atoms were inserted at calculated positions using a riding model.
- [9] G.M. Sheldrick, *SHELXTL* Version 6.12, Bruker AXS, Madison WI, 2001.
- [10] R.C. Mehrotra, R. Bohra, *Metal Carboxylates*, Academic Press Inc., London, 1983.
- [11] Fungal screening. *C. albicans* (ATCC 10231, Manassas, VA, USA.) was grown on Sabouraud dextrose agar (SDA) plates at 37 °C and maintained at 4 °C for short-term storage. Cultures were routinely sub-cultured every 4–6 weeks. Cultures were grown to the stationary phase (approximately 1×10^8 cells cm^{-3}) overnight at 37 °C in minimal medium (2% w/v glucose, 0.5% w/v yeast nitrogen base (without amino acids or ammonium sulphate), 0.5% w/v ammonium sulphate), again at 37 °C. Complexes (0.02 g) were dissolved in DMSO (1 cm^3) and added to water (9 cm^3) to give a stock solution (concentration 2000 $\mu\text{g cm}^{-3}$). Doubling dilutions of these various stock solutions were made to yield a series of test solutions. It is important to note that, in general, the antimicrobial activity of the Ag-containing solutions/suspensions deteriorated markedly even upon storage at 4 °C for short periods. Thus, fresh solutions were prepared immediately prior to testing. Minimum inhibitory concentrations MIC₁₀₀ values (minimum concentration required to inhibit 100% of cell growth) were then determined using the broth microdilution method [12]. Bacterial screening. *E. coli* was obtained from the Clinical Microbiology Laboratory, St. James's Hospital, Dublin, Ireland, and MRSA from Microbiologics, North St. Cloud Mn, USA. Bacteria were maintained on Nutrient Agar plates at 4 °C and cultured in liquid broth (LB) when required. LB was used for the antibacterial testing. LB (13 g) was dissolved in water (1 L) in a Duran bottle, and then dispensed into 250 cm^3 conical flasks, autoclaved and allowed to cool. Solutions of silver complexes were prepared by dissolving the complex (0.02 g) in DMSO (0.5 cm^3). To this solution was added sterilised Millipore water (9.5 cm^3) to produce a stock solution of concentration 2000 $\mu\text{g cm}^{-3}$. Stock solution (0.5 cm^3) was added to sterile water (9 cm^3) to produce a drug solution of concentration 100 $\mu\text{g cm}^{-3}$ with the concentration of DMSO being 0.5%. This solution (100 μl) was added to a microtiter plate. 1:1 serial dilutions were made so as to produce a test concentration range of 50–0.1 $\mu\text{g cm}^{-3}$. Both *E. coli* and MRSA were grown in LB at 37 °C and 200 rpm to an OD₆₀₀ of 1.0. The microtiter plate was inoculated with 100 μl of bacterial cells (OD₆₀₀ = 1.0). The plates were incubated at 37 °C for 24 h and OD₆₀₀ values were read using an RMX plate reader (USA) to give MIC₅₀ values (minimum concentration required to inhibit 50% of cell growth). Experiments were performed in triplicate and the data analysed using Microsoft Excel.

- [12] M. McCann, M. Geraghty, M. Devereux, D. O'Shea, J. Mason, L. O'Sullivan, *Metal-Based Drugs* 7 (2000) 185;
B. Coyle, K. Kavanagh, M. McCann, M. Devereux, M. Geraghty, *BioMetals* 16 (2003) 321.
- [13] Anti-cancer cytotoxicity assays were performed using two human-derived malignant model cell lines Both hepatocellular carcinoma (Hep-G₂) and renal adenocarcinoma (A-498) cell lines were purchased from the ATCC. The cells were grown as a monolayer in Eagle's minimum essential medium, supplemented with 2 mM L-glutamine and Earle's balanced salt solution, containing 1.5 g dm⁻³ sodium bicarbonate, 0.1 mM non-essential amino acids, 1.0 mM sodium pyruvate, 100 U cm⁻³ penicillin and 100 µg cm⁻³ streptomycin supplemented to contain 10% (v/v) foetal bovine serum. Cells were grown at 37 °C in a humidified atmosphere in the presence of 5% CO₂ and were in the exponential phase of growth at the time of assay. A 100 µl aliquot of Hep-G₂ and A-498 cells were seeded at a density of 5 × 10⁴ and 2.5 × 10⁴ cells cm⁻³, respectively, into sterile 96 well flat-bottomed plates and grown in 5% CO₂ at 37 °C. Test complexes were dissolved in DMSO and diluted with culture media. The maximum percentage of DMSO present in all wells was 0.2% (v/v). Each drug solution (100 µl) was added to replicate wells (five replicates) in the concentration range of 0.1–500 µM and incubated for 96 h. A miniaturised viability assay using 3-(4,5-dimethylthiazol-2-yl)-2,5-diphenyl tetrazolium bromide (MTT) was carried out according to the method described by Mosman [14]. Following drug incubation, cells were assayed by the addition of 20 µl of 5 mg/ml MTT in 0.1 M phosphate buffer saline (pH 7.4) and incubated for 4 h at 37 °C. The overlying medium was aspirated with a syringe and 100 µl of DMSO was then added to dissolve the formazan crystals. Plates were agitated at high speed in order to ensure complete dissolution of the crystals. The optical density was then measured at 550 nm, and cell viability was expressed as a percentage of solvent-treated control cells. The complete assay was repeated three times giving a total of 15 readings for each concentration. The IC₅₀ was calculated and is defined as the drug concentration (µM) causing a 50% reduction in cellular viability. The significance of any reduction in cellular viability was determined using one-way ANOVA (analysis of variance). A probability of 0.05 or less was deemed statistically significant.
- [14] T. Mosmann, Rapid colorimetric assay for cellular growth and survival: applications to proliferation and cytotoxicity assays, *J. Immunol.* 65 (1983) 55–63.